



Cite this: *Photochem. Photobiol. Sci.*, 2020, **19**, 1189

Femtosecond excited state dynamics of stilbene–viologen complexes with a weakly pronounced charge transfer†

Mikhail V. Rusalov, *^a Valery V. Volchkov, ^a Vladimir L. Ivanov,^a Mikhail Ya. Melnikov,^a Fedor E. Gostev,^b Ivan V. Shelaev,^b Victor A. Nadtochenko, ^{a,b} Artem I. Vedernikov,^c Sergey P. Gromov ^{a,c} and Michael V. Alfimov^c

The femtosecond dynamics of photoinduced electron transfers in supramolecular donor–acceptor complexes between (*E*)-bis(18-crown-6)stilbene (**D**) and tetraperchlorates of 2,7-di(2-ammonioethyl)(2,7-diazapyrenium) (**A1**), 3,3'-(*E*)-ethene-1,2-diylbis[1-(3-ammoniopropyl)pyridinium] (**A2**) and 4,4'-ethane-1,2-diylbis[1-(3-ammoniopropyl)pyridinium] (**A3**) was studied. The acceptors **A2** and **A3** are weak electron acceptors whose first reduction potentials are equal to -1.0 and -1.2 V (Ag), respectively, while **A1** is a strong acceptor with a reduction potential of -0.42 V. It was shown that the back electron transfer time in CT-states of the complexes **D·A2** and **D·A3** is 30–40 ps, which is approximately 50 times greater than the analogous time for the charge transfer complexes studied earlier. The complex **D·A1** is characterized by ultrafast back electron transfer (770 fs). The relaxation pathway of excited states of **D·A1** depends on the wavelength of the excitation light. When excited at 356 nm, the accumulation of a transient locally excited (LE) state with a 250 fs lifetime was observed. But when excited at 425 nm, the formation of the LE-state was not observed.

Received 2nd February 2020,
Accepted 3rd July 2020

DOI: 10.1039/d0pp00034e

rsc.li/ppp

Introduction

Weakly bound donor–acceptor systems, in which organic or metal complexes of a donor and an acceptor are spatially separated by isolating saturated chemical bonds, play an important role in optic molecular sensors,¹ photo- and redox switches and molecular machines,^{2,3} photo-galvanic elements,^{2,4} photo-activated catalysts,⁵ artificial photosynthesis,^{6,7} the detection of DNA damage, and DNA protection from photo-degradation.^{8,9} Donor and acceptor fragments can be covalently bound by means of an oligomeric chain^{10–13} or as a component of supramolecular complexes,^{3,14–20} in particular, by intercalating into DNA.^{21–23}

When the overlap of donor and acceptor electron density, determined by the distance between molecules and their mutual orientation, is sufficient enough, the complexes are colored due to the CT-bands in the visible part of the spectrum.^{4,14,17,18,20} Otherwise, the CT-bands may be absent but their effects are manifested in the NMR spectra,^{24–26} circular dichroism,²⁷ and cyclic voltammograms.²⁶

The most important feature of weakly bound donor–acceptor systems is their ability to perform photoinduced energy and electron transfers at long distances.^{8,10,11,21,23,27}

The process of photoinduced electron transfer is important for solar energy utilization because it leads to the separation of charges and the formation of reactive ion-radicals. The forward electron transfer reaction should occur quickly and with high quantum yield, while the back electron transfer reaction should occur as slowly as possible. By varying the donor, acceptor and separating spacer, one may obtain recombination times of several picoseconds,²³ nanoseconds,^{11,13} microseconds²⁷ or milliseconds.²¹ When assembling donor–acceptor molecules into monolayers or thin films, the lifetime of ion-radical pairs may amount to minutes²⁰ or hours.⁴

Supramolecular donor–acceptor complexes involving bis (crown)stilbene and viologen analogues with terminal *N*-ammonioalkyl groups are interesting objects for research

^aChemistry Department, M. V. Lomonosov Moscow State University, Leninskie Gory 1-3, Moscow 119991, Russian Federation.

E-mail: mvrusalov@yandex.ru; Fax: +7 (495) 9328846; Tel: +7 (495) 9391671

^bN. N. Semenov Institute of Chemical Physics, Russian Academy of Sciences, Kosygina str. 4, Moscow 119991, Russian Federation. Fax: +7 (499) 1378357; Tel: +7 (495) 9397347

^cPhotochemistry Center, Federal Scientific Research Center “Crystallography and Photonics”, Russian Academy of Sciences, Novatorov str. 7A-1, Moscow 119421, Russian Federation. Fax: +7 (495) 9361255; Tel: +7 (495) 9350116

†Electronic supplementary information (ESI) available: Transient absorption spectra of **D**, **A1**, **A2**, **A3**, **D·A1·D** and **D·A3**. See DOI: 10.1039/D0PP00034E

due to their high thermodynamic stability and potential fluorescent molecular sensing of inorganic cations and some organic cations.^{28–37}

Previously, by differential femtosecond absorption spectroscopy, we studied ultrafast photoinduced electron transfer in complexes between the donor (*E*)-bis(18-crown-6)stilbene (**D**) and the acceptors of a series of 1,1'-bis(ammonioalkyl)-4,4'-bipyridinium (**A4**, **A5**)^{38,39} and 4,4'-(*E*)-ethene-1,2-diylbis[1-(ammonioalkyl)pyridinium] (**A6**, **A7**).^{32,40,41} The characteristic time of back electron transfer in MeCN for the complexes in a 1 : 1 ratio with 2-ammonioethyl *N*-substituent (**D**·**A4**, **D**·**A6**) was about 400 fs. The analogous time for the complexes with 3-ammonioethyl *N*-substituent (**D**·**A5**, **D**·**A7**) was about 500 fs. The absorption spectra of these complexes exhibits a distinguishable wide CT-band ($\epsilon = 200\text{--}400\text{ M}^{-1}\text{ cm}^{-1}$) with a maximum at 500–550 nm.

The purpose of the present work is to study the spectral-luminescence properties and the dynamics of the excited states of supramolecular charge transfer complexes, which are formed by weak electron acceptors. We used new acceptor compounds, namely, tetraperchlorates of 2,7-di(2-ammonioethyl)(2,7-diazapyrenium) (**A1**), 3,3'-(*E*)-ethene-1,2-diylbis[1-(3-ammoniopropyl)pyridinium] (**A2**), and 4,4'-ethane-1,2-diylbis[1-(3-ammoniopropyl)pyridinium] (**A3**). The compounds **A2** and **A3** are weak electron acceptors, whose first reduction potentials (−0.94 V and −1.17 V relative to the saturated silver chloride electrode, respectively)³⁰ are significantly lower than the reduction potentials of earlier studied homologues **A4**, **A5** (−0.4 V)³⁷ and **A6**, **A7** (−0.5 V).³⁰

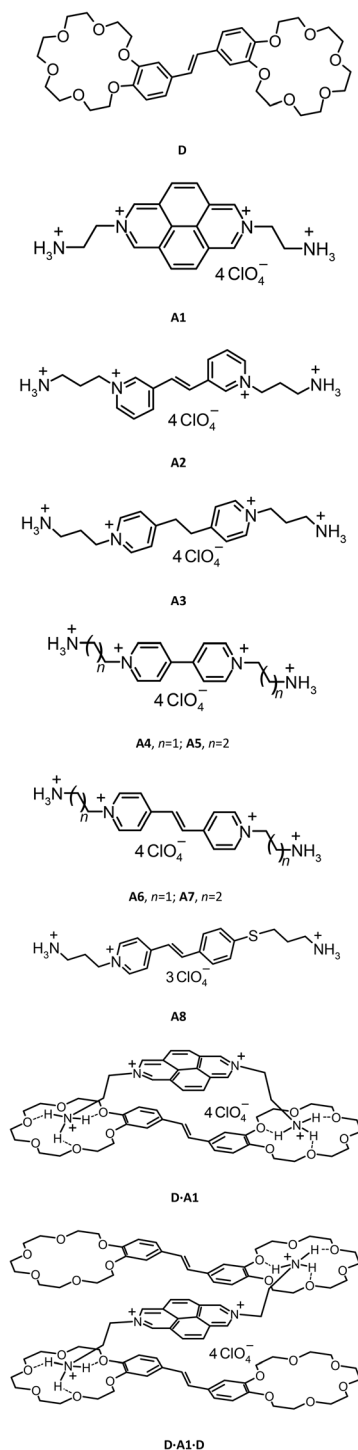
It is known that the electronic spectra of pyrene and other condensed hydrocarbons have a pronounced vibrational structure.^{42,43} Therefore, one can expect that the study of *N,N'*-substituted 2,7-diazapyrenium (**A1**) will provide additional information about the effects the structure of these compounds have on the dynamics of photoinduced electron transfer.

Results and discussion

Steady-state spectroscopy

Fig. 1 shows absorption spectra of compounds **D**, **A1**, **A2**, and **A3**, of the complexes **D**·**A1**, **D**·**A2**, **D**·**A3**, and, partially, **D**·**A1**·**D** (inset I), as well as the longwave part of the spectra of the complexes in 1 : 1 and 2 : 1 ratios (inset II). Normalized fluorescence spectra of **D**, **A1**, **A2** and **A3** are shown as dashed lines. The shortwave part of the absorption spectra of the complexes in 2 : 1 ratios is not shown because they require a great excess of the donor **D**, which has its own absorption in that region. The complex formation of **D** with **A1**, **A2**, and **A3** leads to a small hypsochromic shift of the **D** absorption maximum and to a small bathochromic shift of the first **A1** absorption maximum (Table 1).

In the case of bipyridyl derivatives (**A4**, **A5**) and dipyrindyl-ethylene derivatives (**A6**, **A7**),^{32,38–41} a weak absorption of CT-bands is observed. At the same time, in all cases except for



D·**A1**·**D**, CT-bands manifest themselves as a weak shoulder to the main absorption bands. For this reason, we used Gaussian deconvolution of the CT-bands to obtain their characteristics (Table 2).

By comparing the data from Table 2 with those from prior work,³⁹ one notices a hypsochromic shift of the CT-band maxima of **D**·**A1** and **D**·**A1**·**D** towards the CT-band maxima of the complexes **D**·**A4** and **D**·**A4**·**D** by 3 nm and 43 nm, respectively. Similarly, the hypsochromic shift of the CT-band maxima of **D**·**A2** and **D**·**A2**·**D** towards the CT-band maxima of

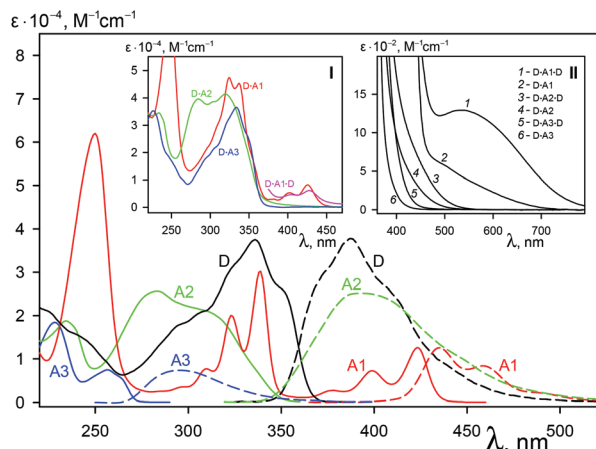


Fig. 1 Absorption spectra (solid lines) and fluorescence spectra (dash lines) of the compounds **D**, **A1**, **A2** and **A3** in MeCN. Inset I: Absorption spectra of the complexes **D-A1**, **D-A2**, **D-A3** and the fragment of **D-A1-D** absorption spectrum in MeCN. Inset II: CT-bands in the absorption spectra of the complexes 1 : 1 and 2 : 1.

Table 1 Wavelength of the first absorption maximum λ_{abs} , molar absorption coefficient ϵ at maximum, wavelength of fluorescence maximum λ_{flv} and fluorescence quantum yield ϕ of the compounds **D**, **A1**, **A2**, and **A3** and some of their complexes in MeCN

	λ_{abs} , nm	ϵ , $\text{M}^{-1} \text{cm}^{-1}$	λ_{flv} , nm	ϕ
D	336	37 500	386	0.39
A1	423	14 000	434	0.31
A2	283	24 000	389	0.26
A3	256	7800	295	<0.001
D-A1	425	8200	— ^a	
D-A1-D	427	6100	— ^a	
D-A2	320	41 500	— ^a	
D-A3	334	36 500	381	0.04

^a Weak fluorescence of the solutions was referred to as residual quantities of initial compounds.

Table 2 Wavelength of maximum λ_{abs} , molar absorption coefficient ϵ_{max} , width at the half-height $\Delta\nu_{1/2}$ of the CT-bands of the complexes 1:1 and 2:1, obtained by the Gaussian deconvolution, their stability constant $\log K$ and the substitution constant $\log K_s$

	ϵ_{max} , $\text{M}^{-1} \text{cm}^{-1}$	λ_{abs} , nm	$\Delta\nu_{1/2}$, cm^{-1}	$\log K$, M^{-1}	$\log K_s$
D-A1-D	1290	556	5590	3.32	
D-A1	376	526	4050	7.68	0.91
D-A2-D	806	410	3900	2.16	
D-A2	490	397	3380	8.72	-0.13
D-A3-D	1160	393	1810	2.51	
D-A3	760	377	1740	8.68	-0.09

D-A7 and **D-A7-D** is equal to 111 nm. Thus, this hypsochromic shift shows that the acceptors **A1** and **A2** form the complexes, in which interfragmentary charge transfer is pronouncedly weaker than in the complexes studied earlier. This charge transfer is even weaker in the complexes with the acceptor **A3**,

whose pyridinium rings are connected by the dimethylene bridge.

The interaction of the biscrown-ether **D** with an acceptor **A** (where **A** may be **A1**, **A2** or **A3**) consecutively leads to the formation of the complexes in 1 : 1 (**D·A**) and 2 : 1 (**D·A·D**) ratios.



Fig. 2 shows changes in the longwave part of the **A1** absorption spectrum as **D** is added. When relative donor concentration C_D is less than unity, a monotonous increase in the absorption at 450–750 nm is observed. This supports the formation of highly stable **D·A1**, according to eqn (1). A further increase in the concentration of **D** leads to a bathochromic shift and a significant enhancement of absorption intensity in the longwave part of the spectrum. This is due to the equilibrium displacement towards the formation of **D·A1·D** with a maximum at 556 nm, according to eqn (2). As shown in Fig. 2, a 50-fold excess of **D** is required for 95% of **A1** binding into **D·A1·D**. This points to the weak stability of the complex **D·A1·D**. The stability constant $\log K_2$ of the complex **D·A1·D**, determined by spectrophotometric titration, is equal to 3.32 (Table 2). The ternary structure of complex **D·A·D** was confirmed earlier by Raman spectroscopy³¹ and X-ray structural analysis.³⁵

Because of the high stability constants of complexes in a 1 : 1 ratio (**D·A**), we used spectrofluorometric titration techniques for their determination.

Like the supramolecular complexes studied previously, the complexes **D·A1** and **D·A2** do not fluoresce due to the fast

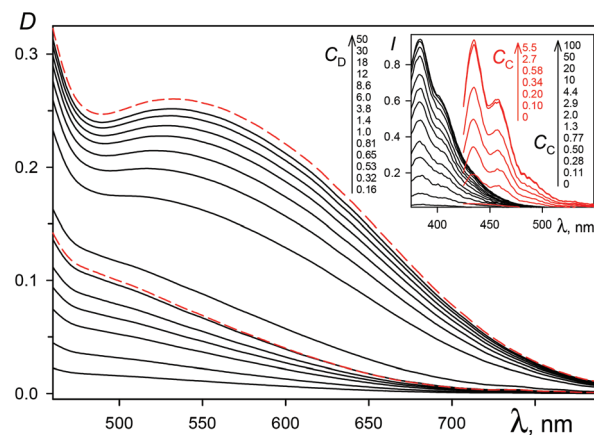


Fig. 2 The dependence of the absorption of MeCN solution of **A1** ($C = 2 \times 10^{-4} \text{ M}$) on the relative concentration of **D** ($C_D = 0.16\text{--}50$). The red dashed lines show the calculated spectra of **D-A1** and **D-A1-D**. Inset: Fluorescence enhancement of MeCN solution of **D-A2** (black lines, $C = 5 \times 10^{-6} \text{ M}$) depending on the relative concentration of 1,12-dodecanediammonium diperchlorate ($C_C = 0\text{--}100$) when excited at 355 nm. Fluorescence enhancement of MeCN solution of **D-A1** (red lines, $C = 5 \times 10^{-6} \text{ M}$) depending on the relative concentration of 1,12-dodecanediammonium diperchlorate ($C_C = 0\text{--}5.5$) when excited at 410 nm.

intramolecular reactions of the forward and back electron transfer, which compete with radiative deactivation. The complex **D·A3** shows weak fluorescence, the maximum of which is shifted by 5 nm in a shortwave range in reference to the fluorescence of **D**. With the gradual addition of the competitor **C**, such as 1,12-dodecanediammonium diperchlorate, non-fluorescent complex **D·A** is destroyed and fluorescent complex **D·C** ($\varphi = 0.58$) forms:



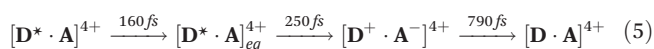
The stability constant K_1 of complexes **D·A** was determined by eqn (4), based on the substitution constant K_S (Table 2) and the known stability constant of **D·C** ($\log K_C = 8.59$).²⁸

$$\log K_1 = \log K_C - \log K_S \quad (4)$$

The black lines in Fig. 2 (inset) show the fluorescence enhancement of the **D·A2** solution as the relative concentration C_C of 1,12-dodecanediammonium diperchlorate increases. Excitation was at 355 nm, where the free acceptor **A2**, formed according to eqn (3), does not absorb light well. The red lines show the fluorescence enhancement of **D·A1** as competitor **C** is added. When excited at 410 nm, the fluorescence of free **A1** with the maximum at 434 nm is observed instead of **D·C** fluorescence. The stability constants of complexes **D·A1** and **D·A2** (Table 2) are close to the earlier obtained values for **D·A4** ($\log K_1 = 7.44$)³⁹ and **D·A7** ($\log K_1 = 9.08$).³² This indicates that supramolecular interaction between ammonioalkyl substituents and crown-ether moieties *via* hydrogen bonds makes the main contribution to the stability of the complexes under study. The contribution of donor–acceptor interaction is small. In series **D·C**, **D·A2** and **D·A7**, a slight growth of the complex stability (8.59, 8.72 and 9.08, respectively) points to a weaker additional donor–acceptor stabilization of **D·A2** as compared to **D·A7**. This may be due to the rotation of the **A2** molecule relative to the plane of the **D** molecule and to a lesser overlap of their electron density as a result of pyridinium ring substitution in the third position.

Transient absorption spectroscopy

Fig. 3 (top panel) shows the dynamics of the transient spectra of **D·A1** ($C = 1.7 \times 10^{-4}$ M) after excitation with a 30 fs, 356 nm laser pulse. The kinetics of the differential optic density changes is satisfactorily described by the sum of three exponents with characteristic times 160 fs, 250 fs and 790 fs (Fig. 3, bottom panel). Similar to the earlier studied complexes of **D** with the acceptors **A4**, **A5**, **A6**, and **A7**,^{32,38–41} one can identify three consecutive stages in the evolution of the transient spectra:



During the first 250 fs after excitation, an accumulation of the relaxed LE-state $[\mathbf{D}^* \cdot \mathbf{A}]_{\text{eq}}^{4+}$ with the absorption maximum at 560 nm takes place by relaxation of the higher lying states with a characteristic time of 160 fs. During the next 200 fs, a hypsochromic shift of the absorption maximum from 560 nm to 510 nm occurs, which corresponds to the conversion of the

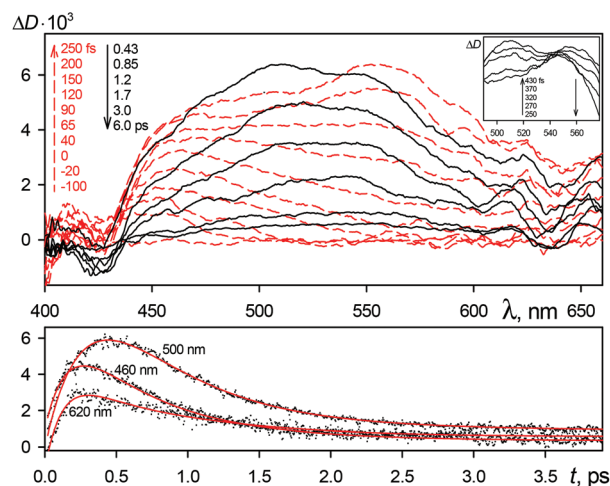


Fig. 3 Top panel: The dynamics of transient absorption spectra of **D·A1** ($C = 1.7 \times 10^{-4}$ M), which correspond to -100 – 250 fs delays (red dashed lines) and to 0.43 – 6.0 ps delays (black solid lines), after the excitation by a 356 nm, 30 fs laser pulse. Inset: The dynamics of **D·A1** spectra near the isosbestic point which correspond to 250 – 430 fs delays. Bottom panel: The kinetic curves of transient absorption spectra for several wavelengths. The red solid lines represent fitting by a three-exponential function with characteristic times of 160 fs, 250 fs and 790 fs.

relaxed LE-state into the CT-state $[\mathbf{D}^+ \cdot \mathbf{A}^-]^{4+}$ with a characteristic time of 250 fs (Fig. 3, inset).

At the final stage, near 6 ps, a decrease of signal level down to a residual value is observed, which corresponds to CT-state decay by its conversion into the ground state $[\mathbf{D} \cdot \mathbf{A}]^{4+}$ with the characteristic time of 790 fs. The residual absorption and stimulated emission at 430 nm were attributed to the S_1 -state of a small amount of free **A1**. Because the absorption spectrum of **A1** and fluorescence spectrum of **D** overlap in the region 380 – 420 nm, the energy transfer from **D** to **A1** cannot be ruled out. However, the complex **D·A1** does not strongly fluoresce, therefore the stimulated emission of a small amount of **A1** can be assigned to the direct excitation of **A1**. The presence of an isosbestic point in Fig. 3 (inset) also indicates that **D*** completely transforms into the CT-state of **D·A1**.

Fig. 4 (top panel) shows the dynamics of the transient spectra of **D·A1** ($C = 5 \times 10^{-4}$ M) after excitation with a 40 fs, 425 nm laser pulse, which corresponds to the longwave maximum of **A1** absorption. The kinetics of the differential optic density changes is satisfactorily described by the sum of two exponents with characteristic times of 160 fs and 740 fs (Fig. 4, bottom panel).

During the first 350 fs after excitation, an intensification of the signal with a maximum at 510 nm takes place, which was attributed to the CT-state absorption. During the next 5 ps, this signal decays to the residual level from the CT-state into the ground state with the characteristic time of 740 fs.

Based on the electron redistribution at the frontier orbitals of the donor and acceptor after excitation, one can identify¹ four types of transfer processes: Förster resonance energy transfer,⁴⁴ LUMO–LUMO, as well as HOMO–HOMO electron transfer,^{4,11,20,21,27} and Dexter electron exchange.^{8,10,12}

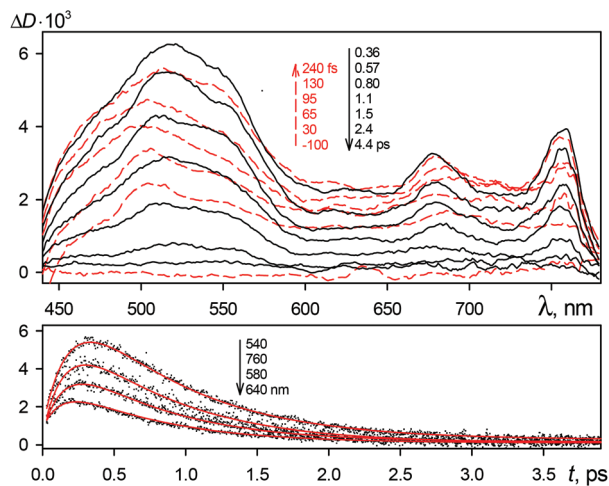
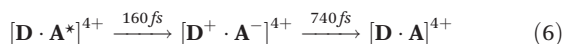


Fig. 4 Top panel: The dynamics of transient absorption spectra of **D-A1** ($C = 5 \times 10^{-4}$ M), which correspond to -100 – 240 fs delays (red dashed lines) and to 0.36 – 4.4 ps delays (black solid lines), after the excitation by a 425 nm, 40 fs laser pulse. Bottom panel: The kinetic curves of transient absorption spectra for several wavelengths. The red solid lines represent fitting by a two-exponential function with characteristic times of 160 fs and 740 fs.

If we compare the dynamics of excited states of **D-A1**, obtained upon the selective excitation of the donor (356 nm) and the acceptor (425 nm), we obtain rather similar values of CT-state lifetimes (790 and 740 fs, respectively) and practically identical absorption spectra of CT-states. However, as is seen from Fig. 4, the accumulation of the relaxed LE-state is not observed. This relationship between the relaxation pathway and the excitation wavelength can be explained by the fact that the forward electron transfer takes place between LUMO–LUMO orbitals upon donor excitation and between HOMO–HOMO orbitals upon acceptor excitation.¹ The processes in Fig. 4 can be written as follows:



The comparison of the dynamics of the **D-A1** excited state with the earlier studied³⁹ complex **D-A4** allows us to identify the following differences. First, the lifetime of the **D-A1** CT-state (770 ± 30 fs) is approximately twice as high as the analogous value for **D-A4** (400 fs). This discrepancy cannot be explained by a difference in the driving force of the back electron transfer reaction, because the values of free Gibbs energy changes (ΔG_0) for **D-A1** and **D-A4** are practically identical (-1.47 eV and -1.46 eV, respectively).³⁷

Secondly, the evolution of **D-A4** excited states does not depend on the wavelength of the exciting light and proceeds through the accumulation of the intermediate LE-state. In the case of **D-A1**, the relaxation pathway depends on the wavelength of the exciting light. When excited at 356 nm, relaxation proceeds through an intermediate LE-state, whereas when excited at 425 nm, LE-state accumulation is not observed. Previously, the absence of the intermediate LE-state in the

dynamics of the excited state of complexes was observed only for **D-A6** and **D-A7** when excited directly at the CT-band (about 600 nm).^{32,40}

In order to identify the absorption spectra of individual components, the experimental matrix of differential optical densities $\Delta D(\lambda, t)$ was presented as a linear combination of Species Associated Spectra $\varepsilon_i(\lambda)$ (SAS):

$$\Delta D(\lambda, t) = \varepsilon_0(\lambda) + \sum_{i=1}^4 \varepsilon_i(\lambda) C_i(t, \tau_1, \tau_2, \tau_3, \tau_4) \quad (7)$$

Here, $\Delta D(\lambda, t)$ is an experimental matrix of differential optical densities, depending on wavelength λ and time t ; $\varepsilon_i(\lambda)$ is a time independent absorption spectrum of the i -th component, $\varepsilon_0(\lambda)$ is residual absorption; $C_i(t, \tau)$ is the time dependent concentration of the i -th component.

The time profiles $C_i(t, \tau)$ were calculated by solving the system of differential equations according to eqn (8):

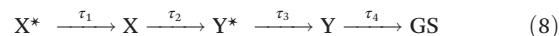


Table 3 shows the values of characteristic times τ_i corresponding to eqn (8) for various compounds. The empty cells are left empty for those cases when the corresponding intermediate product is not accumulated and does not manifest itself in the transient absorption spectra. \mathbf{X}^* denotes the initial short lived non-relaxed excited states, the relaxation of which over 50 – 200 fs leads to the growth of the initial absorption. These times are significantly greater than the growth time of the front of the exciting laser pulse (10 fs). Thus, these times cannot be explained exclusively by the effects of the Instrumental Response Function (IRF).

\mathbf{X} denotes the relaxed LE-states, which were observed in the dynamics of the transient spectra of **A1**, **D-A1** and **D-A3**. The criterion of referring the spectral component \mathbf{X} to the LE-state was the significant difference of its spectrum shape and position from the spectrum of the long-lived component \mathbf{Y} . Contrary to this, the spectra of \mathbf{Y}^* are barely different from the spectra of \mathbf{Y} . Therefore, the process of transformation of \mathbf{Y}^* into \mathbf{Y} was referred to as the additional relaxation of \mathbf{Y} .

Table 3 Wavelengths of exciting pulse λ_{ex} , decay times τ_1 – τ_4 according to eqn (8). The empty cells show that a given intermediate product is not accumulated

	λ_{ex} , nm	τ_1 , ps	τ_2 , ps	τ_3 , ps	τ_4 , ps
D	330	0.056		0.24	640^a
A1	320	0.080	0.17	1.5	2700^a
A2	320	0.070		1.9	700^a
A3	260	0.061		2.6	770^a
D-A1	356	0.16	0.25		0.79
	425	0.16			0.74
D-A1-D	425	0.15			0.75
D-A2	356	0.068		0.32	30
D-A3	330	0.023	0.10	0.71	37

^a Decay times of nanosecond and subnanosecond components may be inaccurate since the registration delay time was restricted by 500 ps.

When studying the relaxation of the S_1 -state of the free base of tetraphenylporphyrin in benzene,⁴⁵ three stages with characteristic times of 100–200 fs, 1.4 ps and 10–20 ps were identified. The fastest stage (100–200 fs) was assigned to the Intramolecular Vibrational Redistribution of energy (IVR). The second stage (1.4 ps) was attributed to the Solvent-induced Intramolecular Vibrational Redistribution of energy (SIVR), which takes place due to the elastic collisions with solvent molecules. The third stage (10–20 ps) was attributed to the establishment of thermodynamic equilibrium due to non-elastic molecular collisions.

Therefore, the relaxation process with the characteristic time τ_3 could be referred to as induced vibrational relaxation, caused by the quasi-elastic collisions of excited molecules with solvent molecules. A fast relaxation process, which takes place in the S_1 -states of styryl dyes over 1–2 ps after excitation, was referred to as a solvate relaxation phenomena.⁴⁶ So, the characteristic time τ_3 could also be attributed to the reorganization of the solvate shells.

The long-lived states of the compounds **D**, **A1**, **A2** and **A3** with lifetimes 0.6–2.7 ns were referred to as the first singlet S_1 state. The long-lived states of the complexes **D·A1**, **D·A1·D**, **D·A2** and **D·A3** with lifetimes 0.7–37 ps were referred to as the CT-state.

Because the formation of excimers is possible in the solutions of polycyclic condensed hydrocarbons, it is necessary to consider this possibility since **A1** is a pyrene analogue. For the pronounced formation of excimers by a static mechanism, *i.e.*, by the excitation of ground state aggregates, the concentration of pyrene should be about 10^{-2} – 10^{-1} M.⁴⁷ In the presence of concentrations of pyrene near 10^{-3} – 10^{-2} M, the pronounced formation of excimers takes place by a dynamic mechanism, *i.e.*, by diffusion-controlled collisions of excited molecules with non-excited ones.⁴⁸ During the first 100 picoseconds, the $S_1 \rightarrow S_n$ absorption spectrum of pyrene does not change.⁴⁹ Excimer formation is observed with delays of several nanoseconds or several tens of nanoseconds.^{48,50} Because the concentration of **A1** (2×10^{-4} M) and the delay interval (0–500 ps) in our experiment was about 10 times less than those, which are necessary for the confident observation of pyrene excimers, the formation of excimers should not affect the evolution of the transient absorption spectra.

Fig. 5 shows the absorption spectra of the excited states X and Y according to eqn (8), calculated by the linear least square method, for the initial compounds (top panel) and for a number of their complexes (bottom panel). As shown in Fig. 5, the absorption spectra of CT-states of a majority of the complexes have similar shapes and positions. The CT-spectrum of **D·A2** resembles the spectrum of the S_1 -state of **A2**, though the excitation at 356 nm is initially localized on the donor. The spectra of the LE-states of the compounds **A1** and **D·A1** have a pronounced vibrational structure and drastically differ from the spectra of the long-lived states of these compounds.

The spectrum of the LE-state of **D·A3** reminds the spectrum of the S_1 -state of **D**, but it is red shifted by 20 nm and does not have the band of stimulated emission.

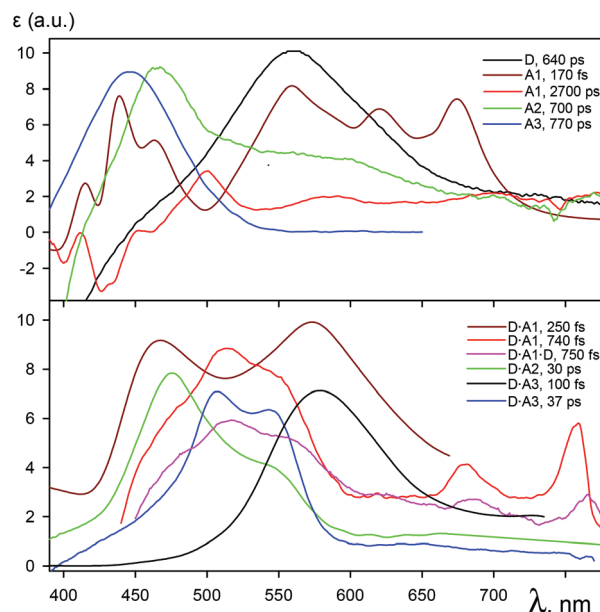


Fig. 5 The absorption spectra of the excited states of **D**, **A1**, **A2**, and **A3** (top panel) and some complexes (bottom panel) with the indication of their lifetimes according to Table 3.

The negative absorption in the $S_1 \rightarrow S_n$ spectra of **D**, **A1** and **A2** (Fig. 5) takes place in the fluorescence region of these compounds (near 385, 435 and 390 nm, respectively) and is caused by stimulated emission.

The transient spectra of **D·A1·D** were obtained in conditions of 50-fold excess of **D**, when the initial acceptor **A1** was almost completely transformed into **D·A1·D**. The excitation was performed at 425 nm, where **D** does not absorb light.

A wave-like artifact caused by the imprint of the second harmonics of the pump pulse is observed in the longwave part of the transient absorption spectra in Fig. 3. Since this artifact is present at some negative delays, we were able to subtract it from the resulting LE-state spectrum of **D·A1** with a 250 fs decay time in Fig. 5.

Fig. 6 (top panel) shows the dynamics of the transient spectra of **D·A2** ($C = 4 \times 10^{-4}$ M) after excitation with a 30 fs, 356 nm laser pulse. The kinetics of the differential optic density changes is satisfactorily described by the sum of three exponents with characteristic times of 68 fs, 320 fs and 30 ps (Fig. 6, bottom panel).

Because, during the relaxation, the spectrum shape changes insignificantly, the intermediate state with a 320 fs lifetime was referred to as the non-relaxed CT*-state. Thus, these processes can be written as follows:



During the first 270 fs after excitation, an accumulation of the non-relaxed CT*-state by the relaxation of the higher lying LE*-states with a characteristic time of 68 fs was observed.

During the next few picoseconds, a certain redistribution of the spectrum intensities at 470 and 550 nm in favour of the

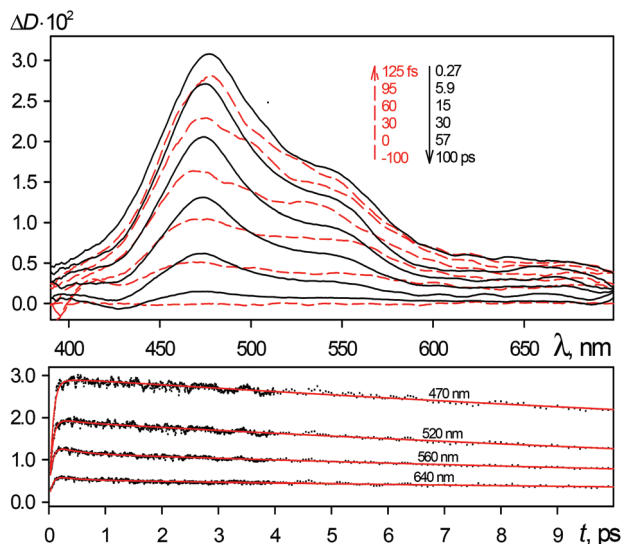


Fig. 6 Top panel: The dynamics of transient absorption spectra of **D-A2** ($C = 4 \times 10^{-4}$ M), which correspond to -100 – 125 fs delays (red dashed lines) and to 0.27 – 100 ps delays (black solid lines), after the excitation by a 356 nm, 30 fs laser pulse. Bottom panel: The kinetic curves of transient absorption spectra for several wavelengths. The red solid lines represent fitting by three-exponential function with characteristic times of 68 fs, 320 fs and 30 ps.

first band takes place. This is caused by the relaxation of the CT*-state into the CT-state with a characteristic time of 320 fs. At the final stage at about 100 ps, a decrease of the signal level down to residual values takes place. This corresponds to the decay of the CT-state into the ground state with a characteristic time of 30 ps.

Because the lifetime of the excited complexes **D-A2** and **D-A3** is approximately 20 times less than the lifetime of the singlet states of **D**, **A2** and **A3**, one can make the conclusion that Förster energy transfer and Dexter electron exchange do not take place. Besides, the fluorescence spectrum of **D** lies in the longwave region as compared with the absorption spectra of **A2** and **A3** and does not intersect them. Therefore, the necessary condition for resonant energy transfer is not observed.

For the quantitative description of the dependence of the reaction rate of back electron transfer on the structure of complexes, we used^{39,40} eqn (10) from Marcus semi-classic single-mode non-adiabatic theory.^{51–53}

$$\frac{1}{\tau_{\text{ET}}} = H_{\text{RP}}^2 \left(\frac{4\pi^3}{h^2 \lambda_1 kT} \right)^{\frac{1}{2}} \sum_{n=0}^{\infty} \frac{S^n}{n!} \exp \left[-S - \frac{(\Delta G_0 + \lambda_1 + n h \nu_a)^2}{4 \lambda_1 kT} \right],$$

$$S = \frac{\lambda_2}{h \nu_a}$$
(10)

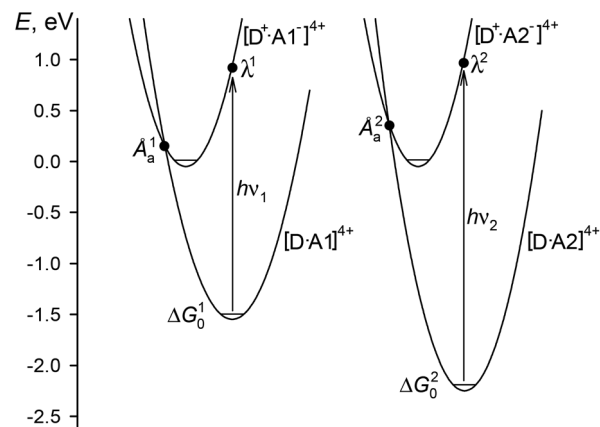
The influence of the complex structure on electron transfer rate is introduced *via* the matrix element of electron overlap H_{RP} , which is calculated from the area of CT-bands and the interplanar distance between the donor and acceptor (4.7 \AA).⁵⁴

For the complexes **D-A7** and **D-A2**, the values of H_{RP} are equal to 0.10 eV and 0.11 eV, respectively, *i.e.*, they practically coincide. The values of the changes in free Gibbs energy ΔG_0 of the back electron transfer for **D-A7** and **D-A2**, obtained from electrochemical data,³⁰ are equal to -1.67 eV and -2.16 eV, respectively. According to Marcus semi-classic theory, when the values of H_{RP} and ΔG_0 are given, the reaction rate is determined by the high-frequency reorganization energy λ_2 . Found from the experimental lifetimes of the CT-states of the complexes **D-A7** and **D-A2** (540 fs and 30 ps, respectively), the values of λ_2 are equal to 0.26 eV and 0.11 eV, respectively. The value of λ_2 for **D-A2** belongs to the interval 0.1 – 0.4 eV, found earlier for analogous supramolecular complexes.³⁹ Hence, one can conclude that a relatively slow rate of back electron transfer in the case of **D-A2** is caused by a high value of the reaction energy effect in the Marcus inverted region.

Scheme 1 shows the harmonic potentials of the initial and final states for a highly exoergic reaction,⁵³ built for the CT-states of **D-A1** and **D-A2**. The energy levels of ground state ΔG_0^1 and ΔG_0^2 (-1.47 and -2.16 eV), energies of total reorganization λ^1 and λ^2 (0.89 and 0.96 eV), and activation energies E_a^1 and E_a^2 (0.09 and 0.38 eV, respectively) are noted in Scheme 1. The values of the total reorganization energies λ were estimated as $\lambda = \Delta G_0 + h \nu_{\text{max}}$, where ν_{max} is a wave number of the CT-band maximum. The values of activation energies E_a were calculated by the Marcus formula⁵³ as $E_a = (\Delta G_0 + \lambda)^2 / 4\lambda$. As shown in Scheme 1, a greater value of $-\Delta G_0$ for **D-A2** as compared to **D-A1** leads to a greater value of activation energy E_a .

Under other equal conditions, the expected increase of electron transfer time when converting from **D-A1** to **D-A2** will be equal to $\exp[(E_a^2 - E_a^1)/k_B T]$. In order to obtain quantitative agreement with the experimental characteristic times of back electron transfer, we made a 14% correction to the estimated values of λ^1 and λ^2 .

In order to describe the deactivation of CT-states of complexes **D-A1**, **D-A1-D**, **D-A2**, and **D-A3** and earlier studied complexes **D-A4**, **D-A4-D**, **D-A5**, **D-A6**, **D-A7**, **D-A7-D**,^{32,38–41} and **D-A8**



Scheme 1 Harmonic potentials of initial and final states for back electron transfer in CT-states of complexes **D-A1** and **D-A2**.

($\tau_{\text{ET}} = 21$ ps),⁵⁵ in terms of general Marcus theory, we used the basic Marcus equation⁵³

$$\frac{1}{\tau_{\text{ET}}} = H_{\text{RP}}^2 \left(\frac{4\pi^3}{h^2 \lambda kT} \right)^{\frac{1}{2}} \exp \left[-\frac{(\Delta G_0 + \lambda)^2}{4\lambda kT} \right] \quad (11)$$

where λ is a total organization energy. The matrix element H_{RP} was estimated by the Hush formula⁵³

$$H_{\text{RP}} = \frac{0.0206}{r} \sqrt{\nu_{\text{max}} \Delta\nu_{1/2} \epsilon_{\text{max}}} \quad (12)$$

Here, ν_{max} , $\Delta\nu_{1/2}$ and ϵ_{max} are the Gaussian parameters, which approximates the CT-band in the absorption spectrum of the complexes, and r is an averaged distance between the donor and acceptor planes.

The wavenumber of the maximum ν_{max} , molar absorption coefficient ϵ_{max} and width at the half-height $\Delta\nu_{1/2}$ of the CT-bands of the complexes were taken from Table 2 and from our previous work.³⁹ The interplanar distance r between the donor and acceptor was assumed to be equal to 3.4 Å for the complexes with an ammonioethyl spacer and 4.7 Å for the complexes with an ammoniopropyl spacer.^{35,37} The values H_{RP} , calculated from eqn (12) vary within 0.10–0.13 eV for the 1 : 1 complexes and 0.18–0.27 eV for the 2 : 1 complexes. The reaction driving force ΔG_0 was calculated as a difference of the first electrochemical potentials E^{red} and E^{ox} of the complexes, by neglecting the Coulomb term.^{30,37} The internal temperature of the CT-states T was fixed at 300 K, assuming its closeness to the bath temperature.³² The total reorganization energy λ was fit in order to ascertain the correlation between the experimental back electron transfer time τ_4 from Table 3 and τ_{ET} according to eqn (11).

Eqn (11) does not describe precisely the experimental values of total reorganization energies $\lambda_{\text{ex}} = \Delta G_0 + h\nu_{\text{max}}$, however, the average value of the experimental total reorganization energy (0.88 ± 0.23 eV) is in good agreement with the average reorganization energy found from eqn (11) (0.89 ± 0.13 eV). Since $-\Delta G_0 > \lambda$, this means that eqn (11) can be used to demonstrate back electron transfer in the inverted Marcus region for all the complexes discussed.

Fig. 7 shows the dependence of the decimal logarithm of the rate constant of back electron transfer k on $\Delta G_0 + \lambda$, where λ was calculated from eqn (11). As shown in Fig. 7, about a 50-fold slowing of the reaction for complexes **D-A2**, **D-A3** and **D-A8** as compared with other complexes is caused by the high exothermic nature of the back electron transfer reaction. This can be explained by the fact that the acceptors **A2**, **A3** and **A8** are weak electron acceptors (reduction potentials are equal to -1.0 , -1.2 , and -0.85 V, respectively). This distinguishes them from the acceptor **A1** with a reduction potential of -0.42 V relative to a silver chloride electrode.³⁷ The process of the back electron transfer in the CT-state of the phthalocyanine-fullerene supramolecular complex also takes place in the inverted Marcus region, where ΔG_0 is equal to -1.1 eV and λ is equal to 0.6 eV.¹³ The small value of total reorganization energy λ was attributed to the spherical symmetry of fullerene.

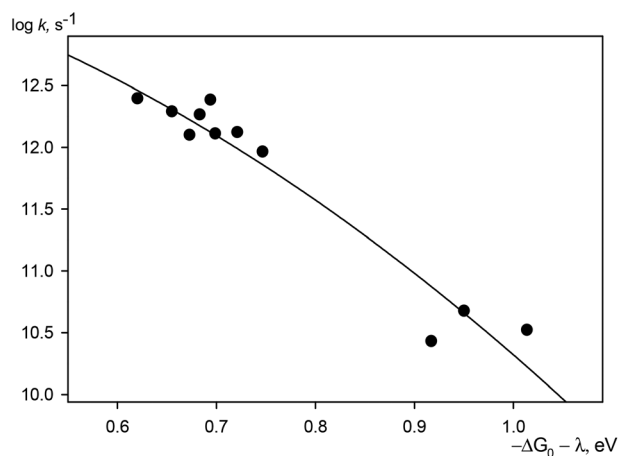


Fig. 7 The dependence of back electron transfer rate constant in CT-states of complexes, formed with acceptors **A1**–**A8**, on the sum of Gibbs energy ΔG_0 and total reorganization energy λ , calculated from eqn (11).

Experimental

(*E*)-Bis(18-crown-6)stilbene (**D**) was prepared according to prior work.⁵⁶ The synthesis of tetraperchlorates of 2,7-di(2-ammonioethyl)(2,7-diazapyrenium) (**A1**), 3,3'-(*E*)-ethene-1,2-diylbis[1-(3-ammoniopropyl)pyridinium] (**A2**) and 4,4'-ethane-1,2-diylbis[1-(3-ammoniopropyl)pyridinium] (**A3**) was carried out as described previously.^{34,37} 1,12-Dodecanediammonium diperchlorate was prepared from the appropriate diamine and 70% perchloric acid (Aldrich) according to prior work.⁵⁷

Anhydrous MeCN (Cryochrom, spectral grade, the water content < 0.03%) was used.

Steady-state absorption spectra were recorded on a Shimadzu-3100 spectrophotometer. Steady-state fluorescence spectra were recorded on a PerkinElmer LS-55 spectrofluorimeter. Fluorescence quantum yields were determined in aerated solutions relative to a solution of quinine bisulfate in 1 N H₂SO₄ ($\phi = 0.546$) used as a standard.⁵⁸

Transient absorption spectra were measured using a femtosecond pump–supercontinuum probe setup. The output of a “Tsunami” Ti/sapphire oscillator (800 nm, 80 MHz, 80 fs, Spectra-Physics, USA) was amplified by a “Spitfire” regenerative amplifier system (Spectra-Physics) at repetition rate 1 kHz. The amplified pulses were split into two beams. One of the beams was directed into a non-collinear phase-matched optical amplifier. A pair of quartz prisms compressed its output, which was centered at 740 nm. The second harmonics was used as a pump pulse. The Gauss pulse of 30 fs at 330 nm or 40 fs at 260 nm was tuned to the pump. The second beam was focused onto a thin quartz cell with H₂O to generate super-continuum probe pulses. The probe pulses were time-delayed with respect to each other. The pulses were then attenuated, recombined, and focused onto the sample cell. The pump and probe light spots had diameters of 300 and 120 μm , respectively. The pump pulse energy was attenuated to 50 nJ to optimize light excitation.

All experiments were carried out at 295 K. Laser pulse frequency was adjusted by a SDG II Spitfire 9132 control amplifier (Spectra-Physics). The pulse operation frequency was 50 Hz. The circulation rate in the flow cell of 0.5 mm thickness was adjusted to avoid multiple excitations. The relative polarization of pump and probe beams was adjusted to 54.7° (magic angle) in parallel and perpendicular polarizations. The super continuum signal out of the sample was dispersed by an Acton SP-300 polychromator and detected by a CCD camera (Roper Scientific SPEC-10). A time correction was applied at each kinetic trace. Control experiments were carried out for non-resonant signals from the pure solvent.

Transient absorption spectra were registered in the 390–780 nm spectral range with a step of 0.43 nm and in a 0–500 ps delay range with a variable step from 3.33 fs to 1000 fs.

The stability constants of the complexes and the characteristic times of the various excited state processes were found by global analysis using the nonlinear least square method with the second order optimization function and Hessian numerical approximation, approaching the calculated matrix of optical densities to the experimental one.⁵⁹

The spectra of individual components *I* were calculated by the linear least square method from the experimental matrix of optic densities *D* and the calculated matrix of concentration profiles *C*:

$$I = DC^T(CC^T)^{-1} \quad (13)$$

Relative errors for the values of equilibrium constants are estimated as 20%, of fluorescence quantum yields as 10%, and of characteristic times of transient absorption dynamics as 10%.

Conclusion

The spectral and thermodynamic properties of the charge transfer complexes 1:1 (**D**·**A**) and 2:1 (**D**·**A**·**D**) between the electron donor (*E*)-bis(18-crown-6)stilbene (**D**) and the acceptors (**A**) of the following series: tetraperchlorate 2,7-di(2-ammonioethyl)(2,7-diazapyrenium) (**A1**), tetraperchlorate 3,3'-(*E*)-ethene-1,2-diylbis[1-(3-ammoniopropyl)pyridinium] (**A2**) and tetraperchlorate 4,4'-ethane-1,2-diylbis[1-(3-ammoniopropyl)pyridinium] (**A3**). The complexes **D**·**A** are highly stable, but the complexes **D**·**A**·**D** are weakly stable. Due to the better geometric correspondence of the molecules of 3-ammoniopropyl-substituted acceptors with the bis-crowned donor **D**, the stability constants of **D**·**A2** and **D**·**A3** are much higher than those of **D**·**A1**.

Because of the weak electron acceptor properties of **A2** and **A3**, their complexes **D**·**A2**, **D**·**A2**·**D**, **D**·**A3**, **D**·**A3**·**D** are characterized by weakly pronounced CT-bands, the maxima of which are hidden against the background of a more intense main longwave absorption band. The maxima of these CT-bands are within 380–400 nm, which is shorter by 100–200 nm than the positions of the maxima of the CT-bands of earlier studied complexes with the acceptors **A4**, **A5**, **A6**, **A7**.

The complexes **D**·**A** do not fluoresce well due to the fast forward and back electron transfer reactions, which compete with radiative recombination. The efficiency of fluorescence increases when the alkane diammonium salts are added due to disruption of the non-fluorescent complex **D**·**A**.

By femtosecond transient absorption spectroscopy, we obtained the lifetimes of the CT-states of **D**·**A2** and **D**·**A3** as 30 and 37 ps, respectively, which are 50–70 times higher than the lifetimes of the supramolecular complexes studied prior. Such a slow rate of the back electron transfer reaction was explained by its high energy effect in the conditions of the inverted mode of Marcus theory. Contrary to the complexes studied prior to this study, the formation of an intermediate locally excited (LE) state is not observed in the dynamics of the excited states of **D**·**A2** and is hardly observed in the case of **D**·**A3**. This can be related to the energy proximity of the main absorption bands and CT-bands because the maxima of CT-bands are within the broadened structure of the main bands. The relaxation pathway of the excited states of **D**·**A1** bands depends on the wavelength of exciting light. When excited at 425 nm, the formation of the LE-state was not observed. When excited at 356 nm, the accumulation of the LE-state with a 250 fs lifetime was observed.

Conflicts of interest

The authors declare no conflicts of interest.

Acknowledgements

This work was supported by the Russian Science Foundation (in respect of organic synthesis, project no. 19-13-00020), by the Russian Foundation for Basic Research (project no. 17-03-00595), and by Ministry of Science and Higher Education of the Russian Federation (in respect of the femtosecond pump and probe setup, Government Assignment 0082-2019-0001, registration no. AAAA-A19-119012890064-7).

References

- 1 T. L. Mako, J. M. Racicot and M. Levine, Supramolecular luminescent sensors, *Chem. Rev.*, 2019, **119**, 322–477.
- 2 A. S. Lukas and M. R. Wasielewski, Approaches to a molecular switch using photoinduced electron and energy transfer, in *Molecular Switches*, ed. B. L. Feringa, Wiley-VCH Verlag, GmbH, 2001, pp. 1–36.
- 3 T. Nabeshima and D. Nishida, Control of binding affinity to paraquat by novel macrocyclic systems responding to redox reactions, *Tetrahedron Lett.*, 2002, **43**, 5719–5722.
- 4 J.-Y. Li, M.-L. Peng, L.-P. Zhang, L.-Zh. Wu, B.-J. Wang and Ch.-H. Tung, Long-lived photoinduced charge separation in carbazole-pyrene-viologen system incorporated in Langmuir-Blodgett films of substituted diazacrown ethers, *J. Photochem. Photobiol., A*, 2002, **150**, 101–108.

- 5 N. A. Romero and D. A. Nicewicz, Organic photoredox catalysis, *Chem. Rev.*, 2016, **116**, 10075–10166.
- 6 A. C. Benniston and A. Harriman, Artificial photosynthesis, *Mater. Today*, 2008, **11**, 26–34.
- 7 M. D. Kärkäs, E. V. Johnston, O. Verho and B. Åkermark, Artificial photosynthesis: from nanosecond electron transfer to catalytic water oxidation, *Acc. Chem. Res.*, 2014, **47**, 100–111.
- 8 L. Antusch, N. Gaß and H.-A. Wagenknecht, Elucidation of the Dexter-type energy transfer in DNA by thymine-thymine dimer formation using photosensitizers as artificial nucleosides, *Angew. Chem., Int. Ed.*, 2016, **55**, 1–6.
- 9 J. C. Genereux and J. K. Barton, Mechanisms for DNA charge transport, *Chem. Rev.*, 2010, **110**, 1642–1662.
- 10 M. K. Brennaman, C. N. Fleming, Ch. A. Slate, S. A. Serron, S. E. Bettis, B. W. Erickson, J. M. Papanikolas and Th. J. Meyer, Distance dependence of intrahelix Ru^{II}* to Os^{II} polypyridyl excited-state energy transfer in oligoproline assemblies, *J. Phys. Chem. B*, 2013, **117**, 6352–6363.
- 11 J. Chen, M. Kuss-Petermann and O. S. Wenger, Distance dependence of bidirectional concerted proton–electron transfer in phenol-Ru(2,2'-bipyridine)₃²⁺ dyads, *Chem. – Eur. J.*, 2014, **20**, 4098–4104.
- 12 A. Nielsen, G. Kuzmanich and M. A. Garcia-Garibay, Solid state and their distance-dependence in solution reveal a Dexter S₂–S₂ energy-transfer mechanism, *J. Phys. Chem. A*, 2014, **118**, 1858–1863.
- 13 F. D'Souza, E. Maligaspe, A. S. D. Sandanayaka, N. K. Subbaiyan, P. A. Karr, T. Hasobe and O. Ito, Photochemical charge separation in supramolecular phthalocyanine-multifullerene conjugates assembled by crown ether-alkyl ammonium cation interactions, *J. Phys. Chem. A*, 2010, **114**, 10951–10959.
- 14 J.-F. Xu, Y.-Zh. Chen, L.-Zh. Wu, Ch.-H. Tung and Q.-Z. Yang, Synthesis of a photoresponsive cryptand and its complexations with paraquat and 2,7-diazapyrenium, *Org. Lett.*, 2014, **16**, 684–687.
- 15 P. L. Anelli, N. Spencer and J. F. Stoddart, Diazadibenzo-30-crown-10 derivatives as receptors for diquat, *Tetrahedron Lett.*, 1988, **29**, 1569–1572.
- 16 F. Huang, L. N. Zakharov, A. L. Rheingold, M. Ashraf-Khorassani and H. W. Gibson, Synthesis of a symmetric cylindrical bis(crown ether) host and its complexation with paraquat, *J. Org. Chem.*, 2005, **70**, 809–813.
- 17 F. Huang, P. Gantzel, D. S. Nagvekar, A. L. Rheingold and H. W. Gibson, Taco grande: a dumbbell bis(crown ether)/paraquat [3](taco complex), *Tetrahedron Lett.*, 2006, **47**, 7841–7844.
- 18 M. Zhang, K. Zhu and F. Huang, Improved complexation of paraquat derivatives by the formation of crown ether-based cryptands, *Chem. Commun.*, 2010, **46**, 8131–8141.
- 19 R. S. Forgan, Ch. Wang, D. C. Friedman, J. M. Spruell, Ch. L. Stern, A. A. Sarjeant, D. Cao and J. F. Stoddart, Donor–acceptor ring-in-ring complexes, *Chem. – Eur. J.*, 2012, **18**, 202–212.
- 20 T. Kuwabara, M. Sugiyama, K. Takeuchi and H. Sakane, Catenane and inclusion complex as photochromic compounds involving viologen units, *J. Photochem. Photobiol., A*, 2013, **269**, 59–64.
- 21 A. M. Brun and A. Harriman, Dynamics of electron transfer between intercalated polycyclic molecules: effect of interspersed bases, *J. Am. Chem. Soc.*, 1992, **114**, 3656–3660.
- 22 T. Fiebig, Ch. Wan, Sh. O. Kelley, J. K. Barton and A. H. Zewail, Femtosecond dynamics of the DNA intercalator ethidium and electron transfer with mononucleotides in water, *Proc. Natl. Acad. Sci. U. S. A.*, 1999, **96**, 1187–1192.
- 23 A. I. Kononov, E. B. Moroshkina, N. V. Tkachenko and H. Lemmetyinen, Photophysical processes in the complexes of DNA with ethidium bromide and acridine orange: a femtosecond study, *J. Phys. Chem. B*, 2001, **105**, 535–541.
- 24 M. V. Fomina, A. S. Nikiforov, A. I. Vedernikov, N. A. Kurchavov and S. P. Gromov, Self-assembly of supramolecular complexes of cyanine dyes containing terminal ammonium groups with bis(18-crown-6)stilbene, *Mendeleev Commun.*, 2014, **24**, 295–297.
- 25 E. N. Ushakov, T. P. Martyanov, A. I. Vedernikov, S. K. Sazonov, I. G. Strel'nikov, L. S. Klimenko, M. V. Al'fimov and S. P. Gromov, Stereospecific [2 + 2]-cross-photocycloaddition in a supramolecular donor–acceptor complex, *Tetrahedron Lett.*, 2019, **60**, 150–153.
- 26 E. V. Lukovskaya, A. A. Kosmacheva, O. A. Fedorova, A. A. Bobyleva, A. V. Dolganov, N. E. Shepel', Yu. V. Fedorov, V. V. Novikov and A. V. Anisimov, Synthesis of chromophoric crown-containing styryl derivative of terthiophene and its complexation with octane-1,8-diaminium diperchlorate, *Russ. J. Org. Chem.*, 2014, **50**, 552–558.
- 27 M. Sisido, S. Hoshino, H. Kusano, M. Kuragaki, M. Makino, H. Sasaki, T. A. Smith and K. P. Ghiggino, Distance dependence of photoinduced electron transfer along α -helical polypeptides, *J. Phys. Chem. B*, 2001, **105**, 10407–10415.
- 28 E. N. Ushakov, S. P. Gromov, A. I. Vedernikov, E. V. Malysheva, A. A. Botsmanova, M. V. Al'fimov, B. Eliasson, U. G. Edlund, J. K. Whitesell and M. A. Fox, Self-organization of highly stable electron donor–acceptor complexes via host–guest interactions, *J. Phys. Chem. A*, 2002, **106**, 2020–2023.
- 29 S. P. Gromov, E. N. Ushakov, A. I. Vedernikov, N. A. Lobova, M. V. Al'fimov, Yu. A. Strel'enko, J. K. Whitesell and M. A. Fox, A novel optical sensor for metal ions based on ground-state intermolecular charge-transfer complexation, *Org. Lett.*, 1999, **1**, 1697–1699.
- 30 K. P. Butin, A. A. Moiseeva, S. P. Gromov, A. I. Vedernikov, A. A. Botsmanova, E. N. Ushakov and M. V. Al'fimov, Prospects of electroanalytical investigations of supramolecular complexes of a bis-crown stilbene with viologen-like compounds bearing two ammonioalkyl groups, *J. Electroanal. Chem.*, 2003, **547**, 93–102.
- 31 I. S. Alaverdian, A. V. Feofanov, S. P. Gromov, A. I. Vedernikov, N. A. Lobova and M. V. Al'fimov, Structure of charge-transfer complexes formed by bis-crown stilbene

- and dipyriddyethylene derivatives as probed by surface-enhanced Raman scattering spectroscopy, *J. Phys. Chem. A*, 2003, **107**, 9542–9546.
- 32 E. N. Ushakov, V. A. Nadtochenko, S. P. Gromov, A. I. Vedernikov, N. A. Lobova, M. V. Alfimov, F. E. Gostev, A. N. Petrukhin and O. M. Sarkisov, Ultrafast excited state dynamics of the bi- and termolecular stilbene-viologen charge-transfer complexes assembled via host-guest interactions, *Chem. Phys.*, 2004, **298**, 251–261.
- 33 Yu. S. Alaverdyan, A. V. Feofanov, S. P. Gromov, A. I. Vedernikov, N. A. Lobova and M. V. Alfimov, Spectroscopy of surface-enhanced Raman scattering of a complex with charge transfer between a bis-crown-containing stilbene and a bis-ammonium-alkyl derivative of dipyriddyethylene, *Opt. Spectrosc.*, 2004, **97**, 560–566.
- 34 S. P. Gromov, A. I. Vedernikov, E. N. Ushakov, N. A. Lobova, A. A. Botsmanova, L. G. Kuz'mina, A. V. Churakov, Yu. A. Strelenko, M. V. Alfimov, J. A. K. Howard, D. Johnels and U. G. Edlund, Novel supramolecular charge-transfer systems based on bis(18-crown-6)stilbene and viologen analogues bearing two ammonioalkyl groups, *New J. Chem.*, 2005, **29**, 881–894.
- 35 A. I. Vedernikov, L. G. Kuz'mina, N. A. Lobova, E. N. Ushakov, J. A. K. Howard, M. V. Alfimov and S. P. Gromov, Unusual three-decker structure of a D–A–D complex between bis(crown)stilbene and a di(quinolyl)ethylene derivative, *Mendeleev Commun.*, 2007, **17**, 151–153.
- 36 S. P. Gromov, A. I. Vedernikov, E. N. Ushakov and M. V. Alfimov, Unusual supramolecular donor-acceptor complexes of bis(crown)stilbenes and bis(crown)azobenzene with viologen analogs, *Russ. Chem. Bull.*, 2008, **57**, 793–801.
- 37 A. I. Vedernikov, E. N. Ushakov, A. A. Efremova, L. G. Kuz'mina, A. A. Moiseeva, N. A. Lobova, A. V. Churakov, Yu. A. Strelenko, M. V. Alfimov, J. A. K. Howard and S. P. Gromov, Synthesis, structure, and properties of supramolecular charge-transfer complexes between bis(18-crown-6)stilbene and ammonioalkyl derivatives of 4,4'-bipyridine and 2,7-diazapyrene, *J. Org. Chem.*, 2011, **76**, 6768–6779.
- 38 V. V. Volchkov, M. N. Khimich, M. V. Rusalov, F. E. Gostev, I. V. Shelaev, V. A. Nadtochenko, A. I. Vedernikov, S. P. Gromov, A. Ya. Freidzon, M. V. Alfimov and M. Ya. Melnikov, Formation of supramolecular charge-transfer complex. Ultrafast excited state dynamics and quantum-chemical calculations, *Photochem. Photobiol. Sci.*, 2019, **18**, 232–241.
- 39 M. V. Rusalov, V. V. Volchkov, V. L. Ivanov, M. Ya. Melnikov, F. E. Gostev, V. A. Nadtochenko, A. I. Vedernikov, S. P. Gromov and M. V. Alfimov, Ultrafast excited state dynamics of a stilbene–viologen charge transfer complex and its interaction with alkanediammonium salts, *J. Photochem. Photobiol., A*, 2019, **372**, 89–98.
- 40 M. V. Rusalov, V. V. Volchkov, V. L. Ivanov, M. Ya. Melnikov, I. V. Shelaev, F. E. Gostev, V. A. Nadtochenko, A. I. Vedernikov, S. P. Gromov and M. V. Alfimov, Femtosecond excited state dynamics of a stilbene-viologen charge transfer complex assembled via host-guest interactions, *Photochem. Photobiol. Sci.*, 2017, **16**, 1800–1811.
- 41 V. V. Volchkov, M. V. Rusalov, F. E. Gostev, I. V. Shelaev, V. A. Nadtochenko, A. I. Vedernikov, A. A. Efremova, L. G. Kuz'mina, S. P. Gromov, M. V. Alfimov and M. Ya. Melnikov, Complexation of bis-crown stilbene with alkali and alkaline-earth metal cations. Ultrafast excited state dynamics of the stilbene-viologen analogue charge transfer complex, *J. Phys. Org. Chem.*, 2018, **31**, e3759.
- 42 R. Masrat, M. Maswal and A. A. Dar, Competitive solubilization of naphthalene and pyrene in various micellar systems, *J. Hazard. Mater.*, 2013, **244–245**, 662–670.
- 43 M. D'Abramo, M. Aschi and A. Amadei, Theoretical calculation of the pyrene emission properties in different solvents, *Chem. Phys. Lett.*, 2015, **639**, 17–22.
- 44 W. Wei, C. Xu, J. Ren, B. Xu and X. Qu, Sensing metal ions with ion selectivity of a crown ether and fluorescence resonance energy transfer between carbon dots and graphene, *Chem. Commun.*, 2012, **48**, 1284–1286.
- 45 J. S. Baskin, H.-Zh. Yu and A. H. Zewail, Ultrafast dynamics of porphyrins in the condensed phase: I. Free base tetraphenylporphyrin, *J. Phys. Chem. A*, 2002, **106**, 9837–9844.
- 46 N. V. Bashmakova, Ye. O. Shaydyuk, S. M. Levchenko, A. E. Masunov, O. V. Przhonska, J. L. Bricks, O. D. Kachkovsky, Yu. L. Slominsky, Yu. P. Piryatinski, K. D. Belfield and M. V. Bondar, Design and electronic structure of new styryl dye bases: steady-state and time-resolved spectroscopic studies, *J. Phys. Chem. A*, 2014, **118**, 4502–4509.
- 47 O. A. Khakhel, Absorption spectra of pyrene aggregates in saturated solutions, *J. Appl. Spectrosc.*, 2001, **68**, 280–286.
- 48 D. A. Van Dyke, B. A. Pryor, Ph. G. Smith and M. R. Topp, Nanosecond time-resolved fluorescence spectroscopy in the physical chemistry laboratory: formation of the pyrene excimer in solution, *J. Chem. Educ.*, 1998, **75**, 615–620.
- 49 H. Miyasaka, H. Masuhara and N. Mataga, Picosecond absorption spectra and relaxation processes of the excited singlet state of pyrene in solution, *Laser Chem.*, 1983, **1**, 357–386.
- 50 K. Yoshihara, T. Kasuya, A. Inoue and S. Nagakura, Time resolved spectra of pyrene excimer and pyrene-dimethylaniline exciplex, *Chem. Phys. Lett.*, 1971, **9**, 469–472.
- 51 B. S. Brunshwig and N. Sutin, Rate-constant expressions for nonadiabatic electron-transfer reactions, *Comment. Inorg. Chem.*, 1987, **6**, 209–235.
- 52 H. Sumi and R. A. Marcus, Dynamical effects in electron transfer reactions, *J. Chem. Phys.*, 1986, **84**, 4894–4914.
- 53 P. F. Barbara, T. J. Meyer and M. A. Ratner, Contemporary issues in electron transfer research, *J. Phys. Chem.*, 1996, **100**, 13148–13168.
- 54 A. I. Vedernikov, L. G. Kuz'mina, A. A. Botsmanova, Y. A. Strelenko, J. A. K. Howard, M. V. Alfimov and S. P. Gromov, Stacking structures of complexes between bis(crown)azobenzene and a dipyriddyethylene derivative in a

- crystal and in solution, *Mendeleev Commun.*, 2007, **17**, 148–150.
- 55 E. N. Ushakov, T. P. Martyanov, A. I. Vedernikov, S. K. Sazonov, I. G. Strel'nikov, L. S. Klimenko, M. V. Al'fimov and S. P. Gromov, Stereospecific [2 + 2]-cross-photocycloaddition in a supramolecular donor-acceptor complex, *Tetrahedron Lett.*, 2019, **60**, 150–153.
- 56 A. I. Vedernikov, S. S. Basok, S. P. Gromov, L. G. Kuz'mina, V. G. Avakyan, N. A. Lobova, E. Yu. Kulygina, T. V. Titkov, Yu. A. Strel'enko, E. I. Ivanov, J. A. K. Howard and M. V. Al'fimov, Synthesis and structure of bis-crown-containing stilbenes, *Russ. J. Org. Chem.*, 2005, **41**, 843–854.
- 57 S. P. Gromov, A. I. Vedernikov, L. G. Kuz'mina, N. A. Lobova, S. S. Basok, Yu. A. Strel'enko and M. V. Al'fimov, Stereoselective [2 + 2] photocycloaddition in bispseudosandwich complexes of bis(18-crown-6) stilbene with alkanediammonium ions, *Russ. Chem. Bull.*, 2009, **58**, 108–114.
- 58 W. H. Melhuish, Quantum efficiencies of fluorescence of organic substances – effect of solvent and concentration of fluorescence solute, *J. Phys. Chem.*, 1961, **65**, 229–235.
- 59 M. V. Rusalov, Numerical simulation of chemical equilibria and photostationary states using spectrophotometric and spectrofluorometric data, *Russ. J. Gen. Chem.*, 2005, **75**, 351–358.